Geo-Mar Lett (2014) 34:185–198
DOI 10.1007/s00367-013-0353-z

ORIGINAL

Heat flow in the southern Chile forearc controlled by large-scale tectonic processes

Lucia Villar-Muñoz · Jan H. Behrmann · Juan Diaz-Naveas · Dirk Klaeschen · Jens Karstens

Received: 29 May 2013 / Accepted: 5 December 2013 / Published online: 21 December 2013

Abstract Between 33°S and 47°S, the southern Chile forearc is affected by the subduction of the aseismic Juan Fernandez Ridge, several major oceanic fracture zones on the subducting Nazca Plate, the active Chile Ridge spreading centre, and the underthrusting Antarctic Plate. The heat flow through the forearc was estimated using the depth of the bottom simulating reflector obtained from a comprehensive database of reflection seismic profiles. On the upper and middle continental slope along the whole forearc, heat flow is about 30–60 mW m^{-2}, a range of values common for the continental basement and overlying slope sediments. The actively deforming accretionary wedge on the lower slope, however, in places shows heat flow reaching about 90 mW m^{-2}. This indicates that advecting pore fluids from deeper in the subduction zone may transport a substantial part of the heat there. The large size of the anomalies suggests that fluid advection and outflow at the seafloor is overall diffuse, rather than being restricted to individual fault structures or mud volcanoes and mud mounds. One large area with very high heat flow is associated with a major tectonic feature. Thus, above the subducting Chile Ridge at 46°S, values of up to 280 mW m^{-2} indicate that the overriding South American Plate is effectively heated by subjacent zero-age oceanic plate material.

Responsible guest editor: C. Pierre

L. Villar-Muñoz (✉) · J. H. Behrmann · D. Klaeschen · J. Karstens
GEOMAR Helmholtz Centre for Ocean Research,
Wischhofstr 1-3, 24148 Kiel, Germany
e-mail: lvillar@geomar.de

J. Diaz-Naveas
Escuela de Ciencias del Mar, Pontificia Universidad Católica de Valparaíso, Av. Altamirano, 1480 Valparaíso, Chile

Introduction

Subduction zones are the global sinks for lithospheric rocks and fluids, and the sedimentary rocks covering the oceanic crust on the incoming plate are highly porous and fluid-filled. They also contain variable amounts of organic carbon beneath the overriding plate, which is converted to methane and, to a lesser extent, higher hydrocarbons by biogenic or thermogenic processes. In subduction zones, fluids play a key role in the nucleation and rupture propagation of earthquakes, and are a major agent of advective heat transfer from depth to the Earth's surface. Measurements in drillholes by means of near-surface heat flow probes are a first-order data source but often do not provide enough information for the regional analysis of crustal heat flow. On the other hand, gas hydrates occur in vast areas worldwide in sediments beneath continental slopes (e.g. Kvenvolden 1998; Milkov 2004), and their stability relations can serve to estimate geothermal gradients and, thus, heat flow and its regional variations (e.g. Ganguly et al. 2000). Thus, a prominent feature on reflection seismic profiles is the bottom-simulating reflector (BSR) marking the base of the gas hydrate stability zone (e.g. Hyndman and Spence 1992; Berndt et al. 2004); its depth is a constraint for pressure and temperature in the subsurface.

In this paper the results of an analysis of regional crustal heat flow on the southern and central Chilean continental margin between approx. 33° and 47° southern latitude are presented. For this purpose the BSR distribution was used, and the results were calibrated with the help of available independent heat flow data from near-surface probes and drillholes. Here, gas hydrate occurrence is widespread and has been documented in numerous studies dealing with smaller segments of the margin (e.g. Bangs et al. 1993; Bangs and Brown 1995; Froelich et al. 1995; Brown et al. 1996; Grevemeyer and Villinger 2001; Morales 2003; Grevemeyer et al. 2003, 2006; Vargas Cordero 2009;

Vargas Cordero et al. 2010a, 2010b, 2011). However, to date there has not been a coherent evaluation of forearc heat flow on the scale of a large (>1,000 km strike length) segment of the Chile convergent plate boundary. By such an analysis, the following questions can be addressed:

1. What is the relationship between the age of the subducting plate and forearc heat flow?
2. Is heat transfer through the forearc primarily conductive, or is there evidence for focused advective heat transfer through areas of distributed deformation, like fold-fault packages in accretionary wedges, or individual major fault structures?
3. Does BSR occurrence relate to major tectonic features in the forearc and, if so, what is the relation to geological and tectonic structures at depth?

Geological and tectonic setting

The Chilean margin between 32°S–47°S is mostly shaped by the subduction of the oceanic Nazca Plate beneath the South American Plate (Fig. 1a). The present-day rate of convergence is about 66 mm per year, slightly dextrally oblique with an 80° azimuth (Angermann et al. 1999). The age of the subducting Nazca Plate increases northwards of the Chile Triple Junction (e.g. Behrmann et al. 1992, 1994) to about 35 Ma at 32°S, where the Juan Fernandez Ridge merges with the marine forearc (e.g. Tebbens and Cande 1997). The shallow Juan Fernandez Ridge (Fig. 1) comprises a series of seamounts extending for about 900 km in an ENE–WSW direction (von Huene et al. 1997). Where it approaches the Chile trench the ridge forms an efficient barrier for trench-parallel sediment transport from the south, resulting in a trench between 32°S–47°S that is filled with about 1.5–2 km of sediment (Völker et al. 2006) of terrigenous to hemipelagic composition (e.g. Behrmann et al. 1992; Mix et al. 2003; Heberer et al. 2010).

Today, a substantial fraction of the incoming trench sediment along the margin is frontally accreted (e.g. Diaz-Naveas 1999; Geersen et al. 2011a), building an active accretionary prism on the lower continental slope. Some of the sediment, however, is also being subducted and brought to greater depths along with the subducting Nazca Plate (Behrmann and Kopf 2001). Sediment accretion in the study area has likely been active since the late Miocene or early Pliocene, following a period of non-accretion or subduction erosion (e.g. Kukowski and Oncken 2006). The switch from subduction erosion to sediment accretion may have been triggered by the glaciation of the Patagonian Andes that became significant about 6 Ma ago, resulting in an increased sediment flux to the trench (e.g. Bangs and Cande 1997). Seven major submarine canyons are deeply incised in the forearc, and operate as major pathways for sediment transport to the trench. They are directly connected to river systems that drain the Andes and the coastal Cordillera, and form a link to submarine fans in the trench with silt–sand dominated patterns of sedimentation (e.g. Heberer et al. 2010).

In contrast to the tectonic processes generating the very uniform morphology of the oceanic Nazca Plate, those constraining the more complex morphology and structure of the overriding South American Plate vary strongly from north to south, and also show distinct across-slope segmentation (see, for example, Geersen et al. 2011a for detailed description). Here the most important features are briefly reviewed. Viewed in an upslope direction, the south–central Chilean margin is composed of a young (Pliocene) active accretionary prism, an older (Mesozoic) palaeo-accretionary prism that takes the role of a tectonic backstop of the active accretionary wedge, and continental metamorphic basement (e.g. Bangs and Cande 1997; Contreras-Reyes et al. 2010; Geersen et al. 2011a). The active accretionary prism extends upslope from the deformation front to a water depth of about 2,500 m. It is characterized by a sequence of landward-dipping thrust faults that separate individual thrust sheets (Bangs and Cande 1997; Geersen et al. 2011a). Deformation results in a rough seafloor topography. Further upslope, the Mesozoic palaeo-accretionary prism has a much smoother bathymetric expression, mainly due to a cover of 0.5–2 km of slope and shelf sediments. Active faulting there is restricted to relatively few out-of-sequence thrusts or normal faults (Behrmann et al. 1994; Geersen et al. 2011a). Near the Chilean coastline there is a transition in the subsurface from the palaeo-accretionary prism to the continental metamorphic basement.

In addition to the segmentation across the slope, there is a pronounced structural and seismotectonic north–south segmentation along strike of the plate boundary. For the forearc, this has been interpreted in terms of earthquake rupture (Lomnitz 1970; Comte et al. 1986; Campos et al. 2002; Ruegg et al. 2009), seismicity (Bohm et al. 2002; Haberland et al. 2006), the gravity field (Hackney et al. 2006; Tasárová 2007), the distribution and intensity of submarine mass wasting (Geersen et al. 2011b, 2013; Völker et al. 2012), subduction channel thickness and accretionary prism width (Bangs and Cande 1997; Contreras-Reyes et al. 2010; Geersen et al. 2011a), and topography (Rehak et al. 2008). At the southern termination of the study area near the Chile Triple Junction, most of the forearc has been destroyed by erosion due to the subducting Chile Ridge, to be rebuilt further south by sediment offscraping and accretion from the Antarctic Plate (Behrmann et al. 1994; Behrmann and Kopf 2001; Maksymowicz 2013).

Materials and methods

Database

This study is based on multi-channel seismic reflection data collected along numerous profiles during five geophysical

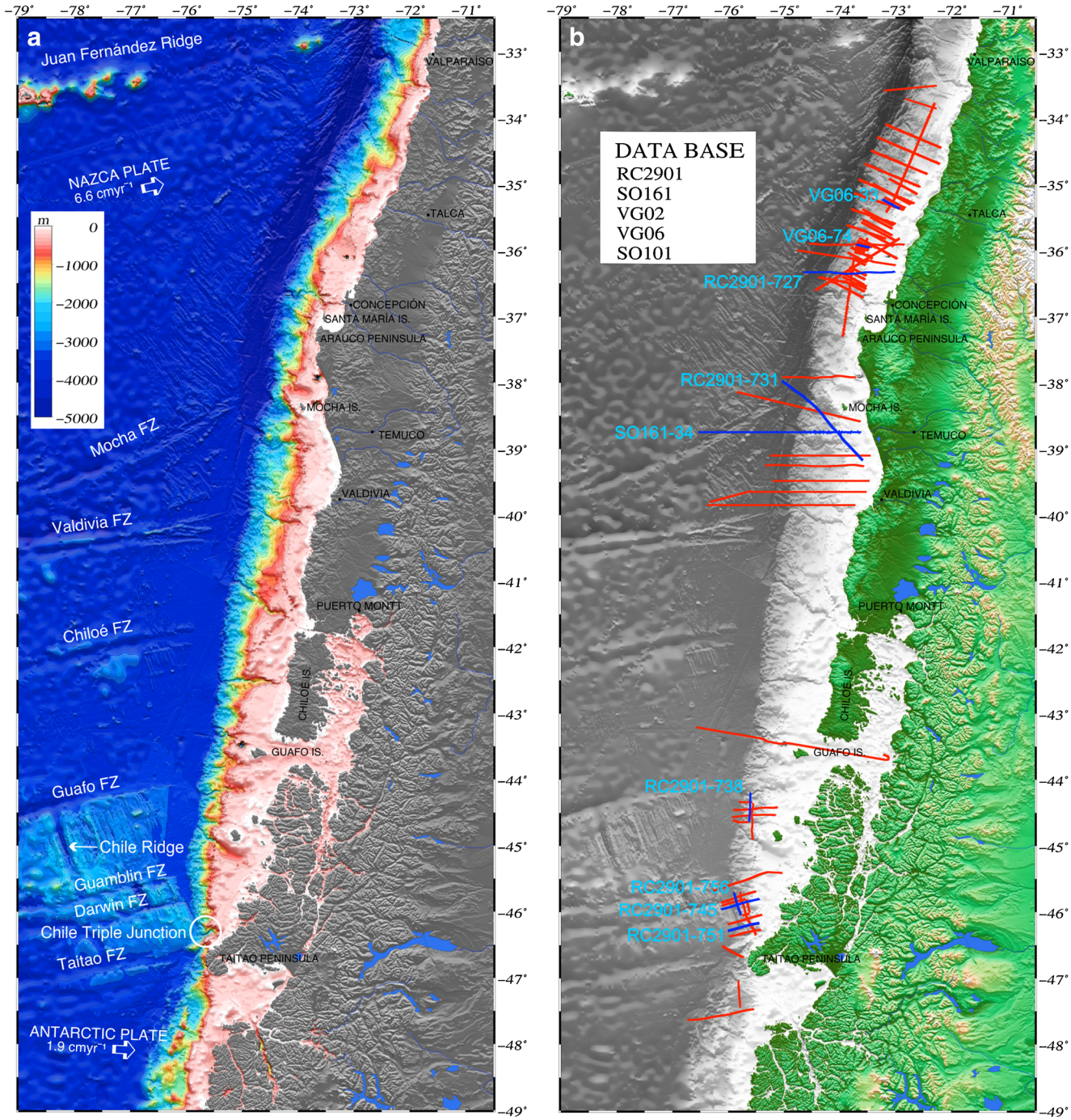

Fig. 1 Location map of the study area offshore Chile, the bathymetry being based on GEBCO_08 Grid (version 20091120, http://www.gebco.net). **a** Tectonic setting of the Nazca, Antarctic and South American plates. Note the aseismic Juan Fernandez Ridge, the fracture zones (FZ) responsible for the age variations of the subducted Nazca and Antarctic plates, and the Chile Ridge today being subducted at 46.4°S. **b** Locations of seismic profiles and ODP legs forming the database used in this study. *Blue lines* Sections presented in other figures

cruises off central–south Chile (32°S–48°S). The locations of all seismic profiles are given in Fig. 1b. Those profiles illustrated in other figures and discussed in more detail are shown in blue, the others in red.

The seismic profiles of research cruise RC2901 aboard R/V Conrad (January–February 1988) were obtained during the "Mid-Ocean Spreading Ridge (Chile Ridge)" project for the Chilean national oil company Empresa Nacional del Petroleo (ENAP), prior to the geophysical survey of the southern Chile margin conducted in preparation for ODP Leg 141 drilling (Bangs and Cande 1997). Most profiles are oriented approx. east–west, perpendicular to the direction of maximum slope

angle (Geersen et al. 2011a); some are oriented parallel to the coast, mainly in the vicinity of the Chile Triple Junction. RC2901 sections were acquired by means of a 3,000-m-long digital streamer, with 240 channels and an intertrace of 12.5 m. A 10-airgun tuned array provided the seismic source, with a total volume of 61.34 l and a shot spacing of 50 m.

R/V Sonne Cruise SO161 of January–February 2001 was carried out within the framework of the "Subduction Processes off Chile (SPOC)" project along the Chile continental margin between 28°S and 44°S, with the general aim of defining the processes and constraints that control the formation of the Chilean continental margin (Reichert et al. 2002). Seismic profiles were acquired using a 3,000-m-long digital streamer with 132 channels. The seismic source was a tuned array of 20 airguns, with a total volume of 51.2 l and a shot spacing of 50 m.

Project SO-101 CONDOR, a study of Chilean offshore natural disasters and ocean environmental research, was carried out in 1995 aboard R/V Sonne. This cruise recovered seismic profiles off the central Chilean forearc.

A research cruise of R/V AGOR Vidal Gormaz was carried out in 2002, as part of the FONDEF Project DOOI104 "Submarine Gas Hydrates: A New Source of Energy for the Twenty-First Century". The primary aim was to locate gas hydrates in sediments along the Chilean margin between 32° and 40°S, at water depths ranging from 200 to 5,000 m (Contardo et al. 2008). A cluster containing four SG-1 sleeve guns with an approximate volume of 40 cubic inches each was used as the seismic source, and a shot spacing of 50 m.

The research cruise VG06 of February 2006 aboard R/V Vidal Gormaz acquired reflection seismic data along the Chilean forearc as part of a second FONDEF project on gas hydrates, the target area being 34°–37°S at 200–3,000 m water depths. The University of Aarhus (Denmark) provided a 600-m-long streamer with 96 channels and an array of four sleeve guns with a total volume of 160 cubic inches. In all, 58 seismic profiles were shot covering an overall length of about 2,350 km (Diaz-Naveas 2007).

Heat flow calculations

Along the central–south Chile continental margin and in similar settings worldwide, commonly occurring BSRs are probably the most widely used indicators for the presence of natural gas hydrates. The reflection is caused by the acoustic impedance contrast between sediments containing gas hydrate and free gas below the gas hydrate stability zone (e.g. Berndt et al. 2004). Thus, BSR imaging of the lower boundary of gas hydrate stability is associated with negative polarity, as can be identified in the seismic sections used in this study (e.g. reflectors imaged in yellow in Fig. 2a and c). Because the stability of gas hydrates is controlled by temperature and pressure conditions (e.g. Grevemeyer et al. 2003), this can serve to calculate the steady-state heat flow q (mW m^{-2}) by using the following formula:

$$q = \frac{T_z - T_0}{\int_0^z \frac{dz'}{k(z')}} \quad (1)$$

where T_z and T_0 are the temperatures at the BSR and the seafloor respectively (Villinger et al. 2010), k is the thermal conductivity and z denotes the BSR depth.

The BSR and the seafloor depths were obtained from the seismic profiles collected during the cruises mentioned above. Seafloor temperatures were taken from CTD measurements off Chile from the World Ocean Data Base (http://www.nodc.noaa.gov/). Thermal conductivity for the southern sector of the study area was taken to be k=1.25 W mK^{-1}, based on drillcore data from ODP Leg 141 (Behrmann et al. 1992; Grevemeyer and Villinger 2001). For the central and northern sectors, thermal conductivity was taken to be k=0.85 W mK^{-1}, based on ODP Leg 202 drillcore data (Grevemeyer et al. 2003; Mix et al. 2003). The differences reflect compositional variations of the sediments and, more importantly, a higher degree of shallow diagenesis in the vicinity of the Chile Triple Junction (see Behrmann et al. 1994). Temperature at the depth of the BSR, T_z, is calculated by using the dissociation temperature–pressure function (Dickens and Quinby-Hunt 1994):

$$1/T = 3.79 \times 10^{-3} - 2.83 \times 10^{-4}(\log p) \quad (2)$$

where p is the hydrostatic pressure (MPa) and T the temperature (Kelvin). Gas in the system is assumed to be pure methane, with a pore water salinity of 35 g l^{-1}. Hydrostatic and lithostatic pressures and depth were calculated by converting the measured TWT (two way travel time) at the BSR using a velocity–depth function derived from the seismic data (Kaul et al. 2000) or, where available, data from ODP drillholes (e.g. Behrmann et al. 1992). To convert water-column TWT into depth, a seawater compressional wave velocity of 1,500 m s^{-1} was used.

Results

A key observation is that the BSR delineating the inferred base of gas hydrates occurs mostly along the 2,000 m water depth contour and is typically located between about 90–630 meters below seafloor (mbsf). For a given water depth, the depth of the BSR below seafloor increases from south to north

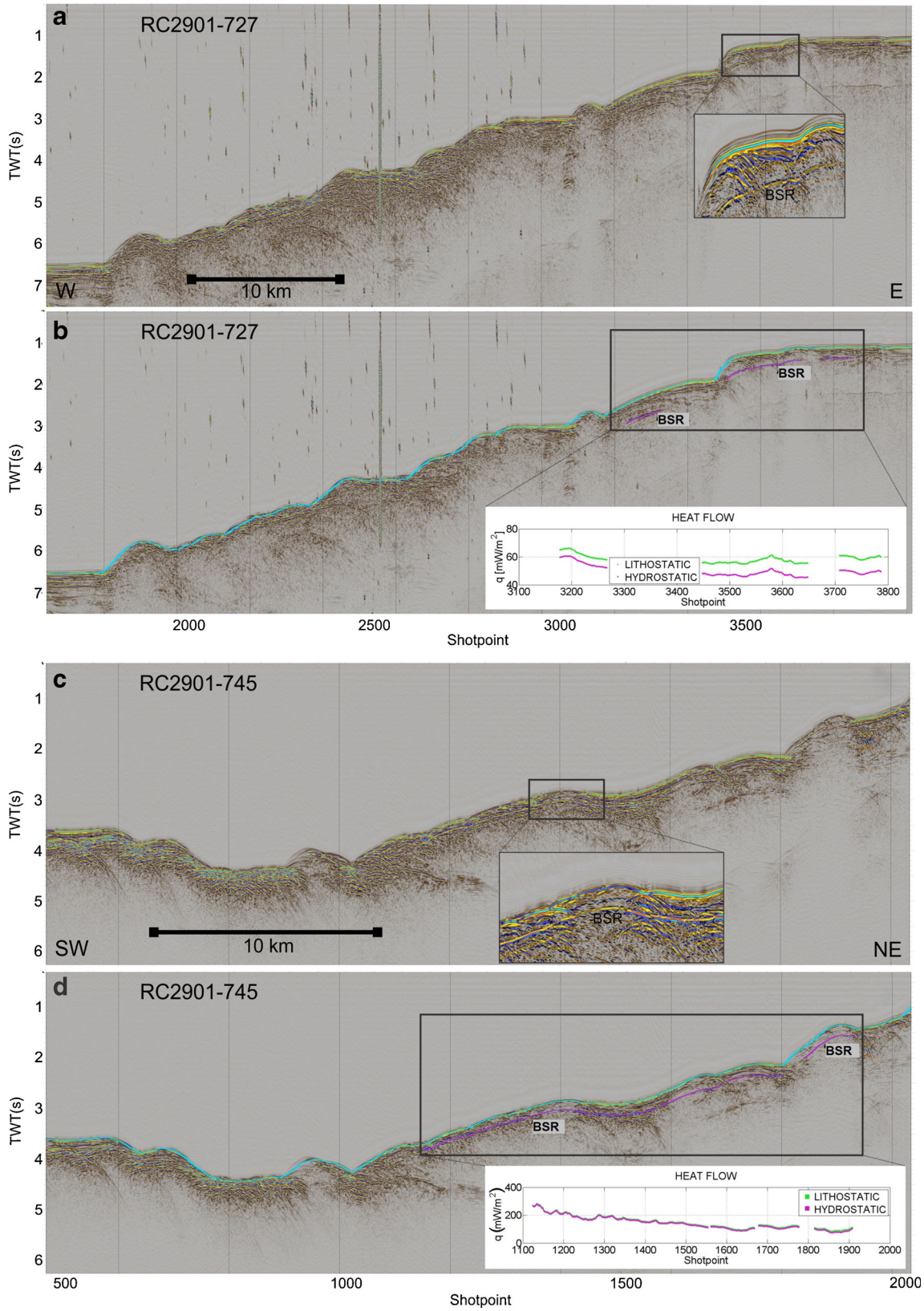

Fig. 2 Two examples of BSR identification. **a** Profile RC2901-727, north sector of study area, zoom showing reverse polarity of BSR (*yellow*). **b** Interpretation of profile RC2901-727 (*purple* BSR), and evaluation of heat flow pattern (*lower right*). **c**, **d** Profile RC2901-745, south sector of study area

in the whole study area (compare Figs. 3a and 4a). The deepest occurrences below seafloor are in deeper waters (>2,000 m) in the northern sector of the study area offshore Valparaiso to Valdivia (33°S–40°S; Fig. 3a). Generally, the BSR shallows upslope above the 2,000 m bathymetric contour in the northern sector, as can be clearly seen in the colour-coded BSR depths (mbsf) reported in Fig. 3a.

On individual seismic profiles in the northern sector of the study area, BSR depth is about 0.3–0.5 s TWT beneath the seafloor. In the three examples given in Fig. 5a–c, this corresponds to heat flows of 30–48 mW m^{-2} for profile SO161-34 (Fig. 5a), 38–60 mW m^{-2} for profile RC 2901-727 (Fig. 5b), and ca. 50 mW m^{-2} for profile RC 2901-731 (Fig. 5c). These values are indicative of conductive heat transfer through forearcs underlain by a relatively old and, therefore, cold subducting oceanic plate. In map view, most of the forearc between 33°S and 40°S is dominated by low heat flow (generally <60 mW m^{-2}).

Distinct deviations from this pattern are rare, and occur at about 35°20′S (offshore Talca), 36°00′S (NW of Concepción) and 38°30′S (SW of Mocha Island). Here heat flow locally increases along section to ca. 90 mW m^{-2}, which is about twice the regional background. The first anomaly is spatially related to a major normal fault scarp (Fig. 6, left-hand panels). The BSR is uplifted on both sides of the fault, and disappears where its projection would intersect the fault plane. BSR uplift is indicative of increased heat flow around the fault trace, and BSR disappearance may be due to inhibition of gas hydrate formation in a zone of vigorous fluid flow along the fault. In the case of the second anomaly (Fig. 6, right-hand panels), the BSR uplift and increased heat flow can be connected to an east-dipping blind thrust that transects the accretionary wedge at depth beneath the forearc cover sediments. The thrust is clearly inactive, as shown by the lack of offset strata in overlying sediments. It may still act as a conduit for fluids from depth, however, creating a local regime of advective heat transfer.

Regarding the third anomaly, the increased heat flow values SW of Mocha Island (Fig. 3b) are in the headscarp area of the southernmost of three large embayments in the forearc slope, where large-scale failure of the forearc slope caused three megascale submarine landslides in the last 600,000 years. The slide that created the southern embayment has a minimum estimated age of 560,000 years and has removed an approx. 500-m-thick section of sediments from the area of increased heat flow (Geersen et al. 2011b). Two explanations are possible for the locally increased heat flow: (1) the headwall of the slide may be an area of fluid advection, or (2) sliding has led to a perturbation of the geothermal gradient in the forearc, which still persists today. On the basis of the available data, it is not possible to decide between these

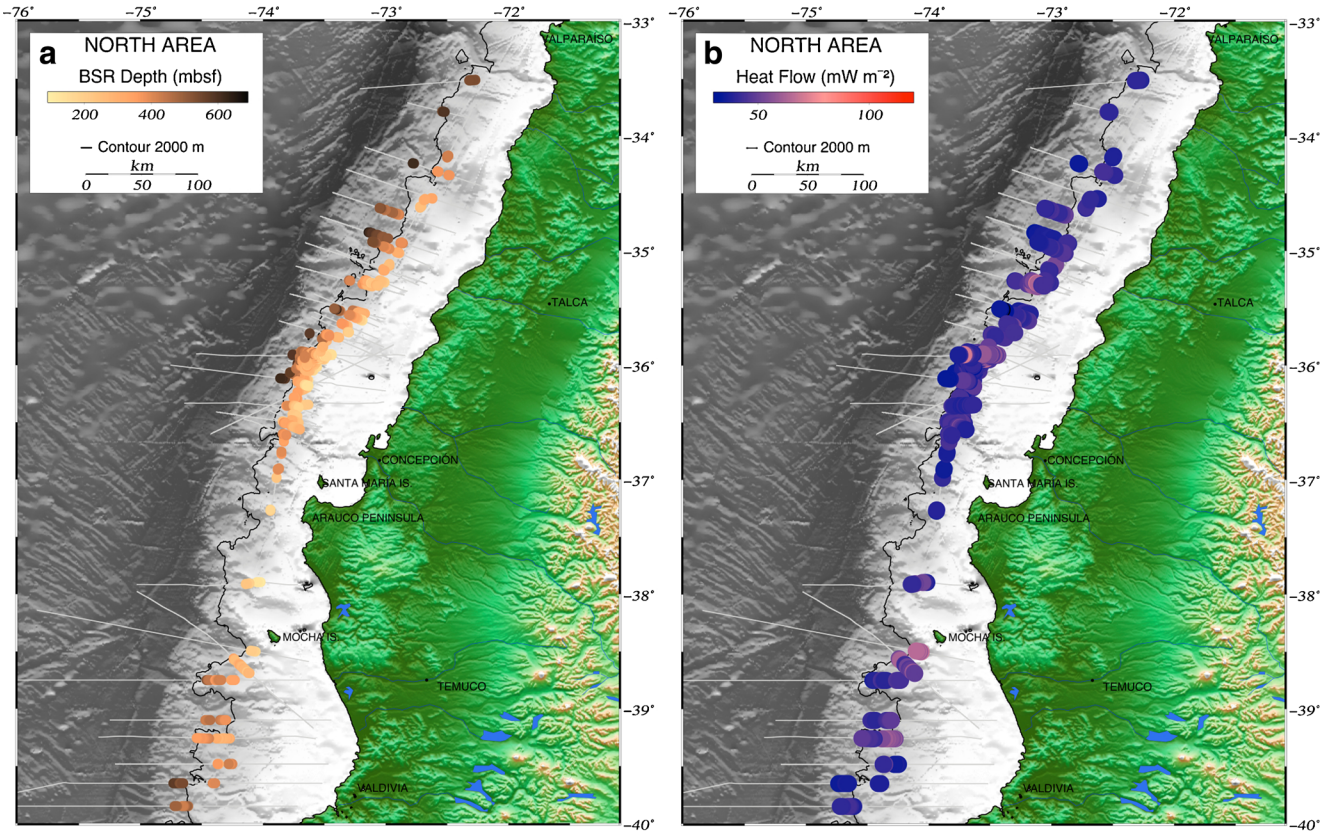

Fig. 3 Large-scale colour-coded results for the northern sector of the study area, based on all seismic profiles available for that sector: **a** BSR depth (mbsf) and **b** heat flow (mW m^{-2}). See text for description

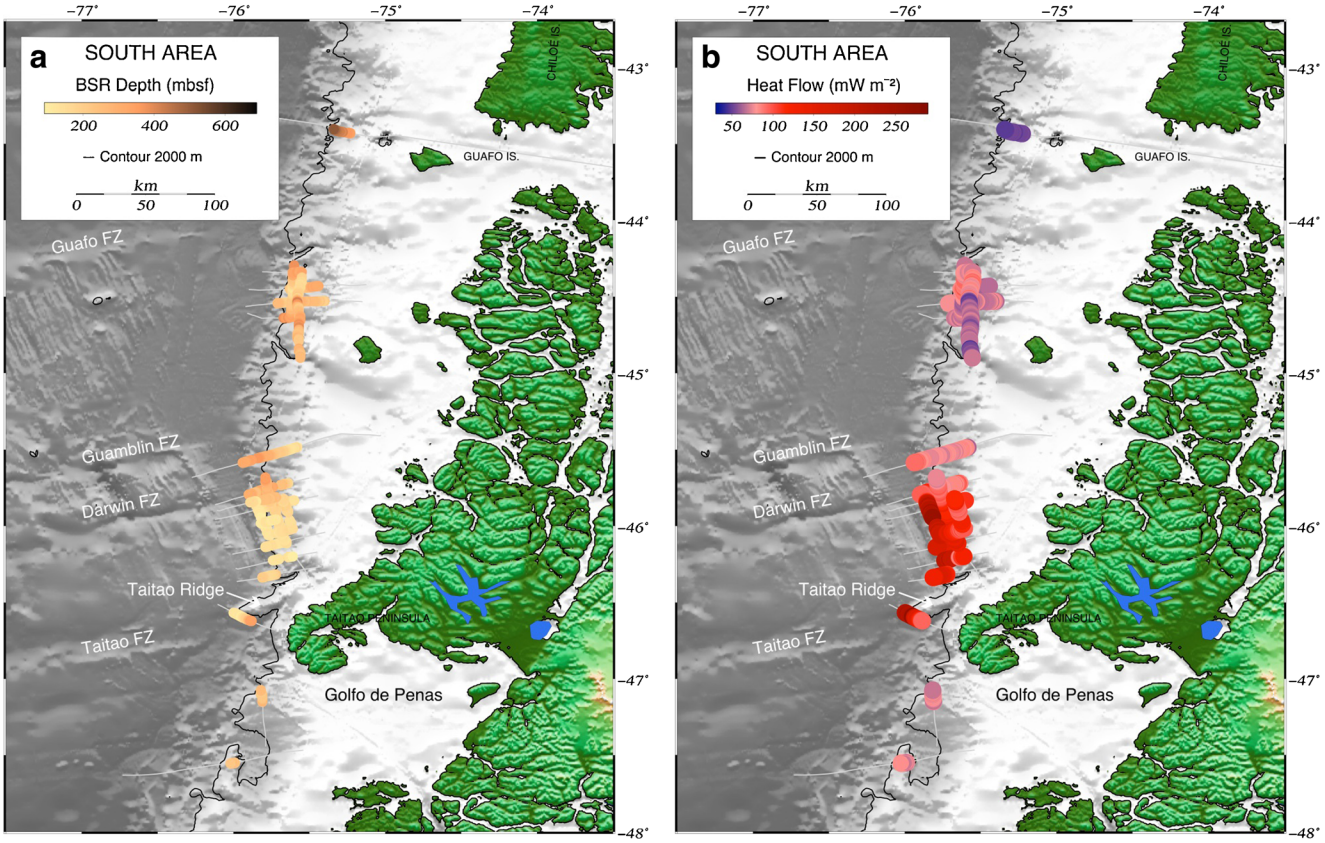

Fig. 4 Large-scale colour-coded results for the southern sector of the study area, based on all seismic profiles available for that sector: **a** BSR depth (mbsf) and **b** heat flow (mW m^{-2}). See text for description

scenarios, but fluid advection and resulting high pore fluid pressures are one major cause for forearc failure discussed in the literature (e.g. Kayen and Lee 1991; Mienert et al. 1998; Behrmann and Meissl 2012). Because BSRs are absent around the central and northern slope embayments of Geersen et al. (2011b), it is impossible to assess the heat flow there and relate it to processes of forearc failure (compare Fig. 3b of this study and Fig. 2 of Geersen et al. 2011b).

In the southern part of the study area between 43°20′S and 47°20′S, the BSR depths below seafloor are generally much larger, irrespective of water depth (see Fig. 3a). Again, BSR occurrence is concentrated along the 2,000 m isobath, mostly slightly above this water depth. Maximum BSR depth is about 500 mbsf in deep water along the seismic profile seawards of Guafo Island at 43°20′S (Fig. 4a). Here the BSR shallows upslope, as one would expect in a regime of constant heat flow along the cross section (compare Fig. 4a and b). Heat flow is low (average of 50 mW m^{-2}) and similar to that of the northern part of the study area (see above).

Between 44°S and 45°S the segment of the Nazca Plate between the Guafo and Guamblin fracture zones is subducted beneath the forearc. Here a cluster of BSRs identified along several seismic profiles shows variable depths, albeit generally shallower than 300 mbsf (Fig. 4a). This corresponds to heat flow values generally not exceeding 100 mW m^{-2}, with an average of 75 mW m^{-2} (Fig. 4b). The example illustrated in Fig. 5d shows an almost continuous BSR along seismic profile RC 2901-738 on the middle forearc slope along strike of the continental margin, the computed heat flow being about 80–100 mW m^{-2}. These higher values are here tentatively explained by the fact that the Nazca Plate oceanic crust being subducted landwards of the Guafo and Guamblin fracture zones is much younger than that being subducted further north (Fig. 1a). South of the landward projection of the Guamblin Fracture Zone, a narrow segment of young Nazca Plate crust is being subducted north of the Darwin Fracture Zone (Fig. 1a). Heat flow values computed from the downslope increasing BSR depths (Fig. 4a) generally lie above 100 mW m^{-2} (Fig. 4b).

South of the Darwin Fracture Zone, the data reveal a pronounced change in BSR characteristics. Here the actively spreading Chile Ridge is subducted beneath the southern Chile forearc. Figure 4a shows that BSR depth decreases southwards along strike of the plate boundary, and also shoals with decreasing water depth. Heat flow is much higher than further northwards, reaching peak values of almost 300 mW m^{-2} (Fig. 4b) at, for example, the western, seaward end of seismic profile RC 2901-745 (Fig. 5e). This is where the eastern flank of the Chile Ridge is today subducting, and the peak values occur at the toe of the accretionary wedge where active deformation and

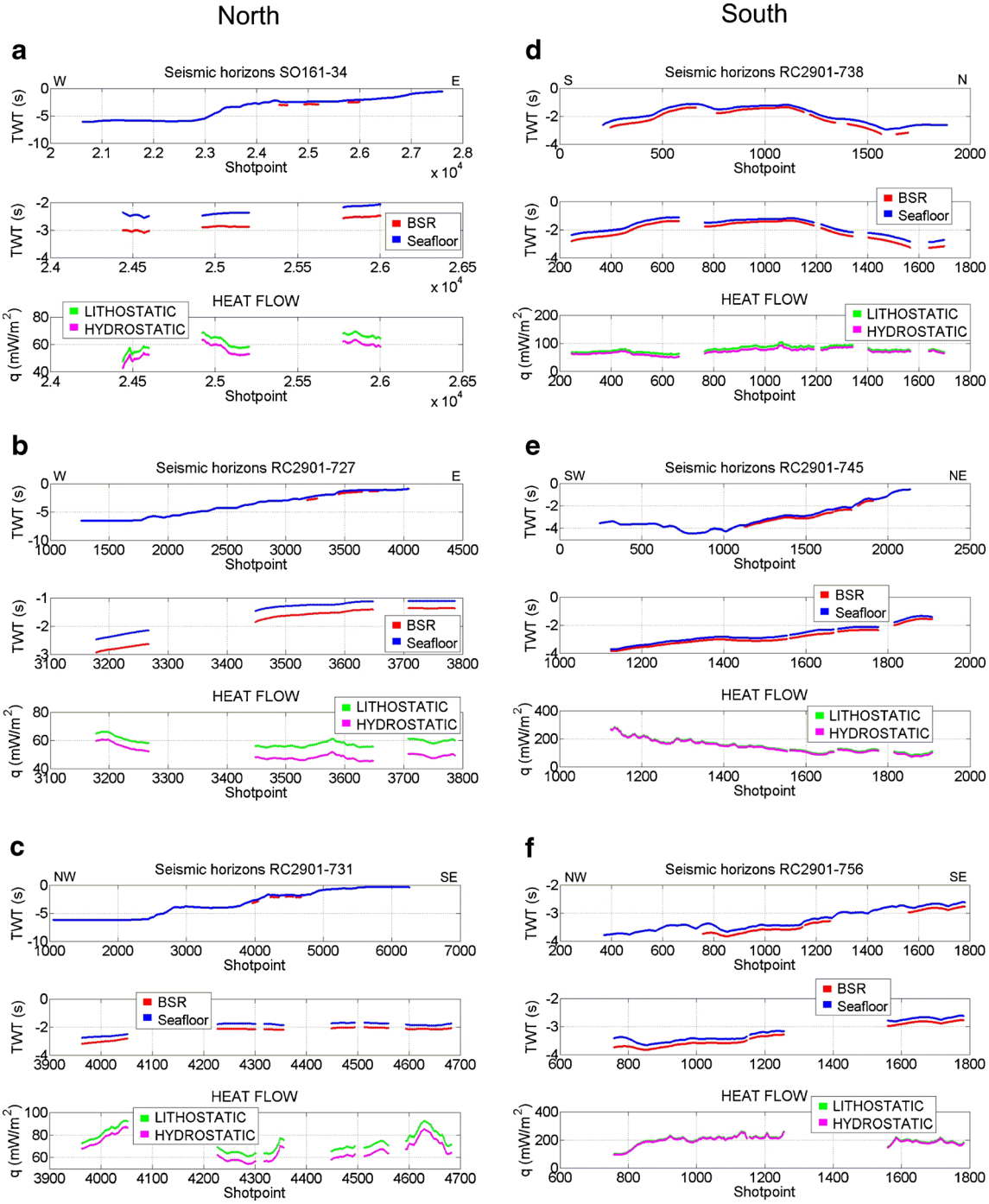

Fig. 5 Examples of calculated heat flow for the northern (**a**–**c**, profiles SO161-34, RC2901-727, RC2901-731) and southern (**d**–**f**, profiles RC2901-738, RC2901-745, RC2901-756) parts of the study area. In each diagram, the upper and middle boxes show the seismic horizons identified for the seafloor (*blue*) and the BSR (*red*), and the lower box the computed heat flow based on assumed lithostatic and hydrostatic pressure

associated fluid flow are most intense. Further upslope heat flow decreases steadily to about 100 mW m^{-2}, probably reflecting the underlying Patagonian forearc basement that is not yet being heated by the subducting oceanic crust. The data for seismic profile RC 2901-756 (Fig. 5f), a strike line that leads gently upslope in a southward direction, show that heat flow along strike of the forearc is generally about 200 mW m^{-2} on the lower forearc slope. Along seismic profile RC 2901-751 (Fig. 7), heat flow is high (ca. 200 mW m^{-2}) above the projected spreading axis of the subducted Chile Ridge. Geothermal gradients measured here by temperature logging in a borehole at ODP Site 863 are as high as 100 °C per km (see Behrmann et al. 1992). Landwards of a major active normal fault that offsets strata and the seafloor, heat flow decreases to about 100 mW m^{-2}.

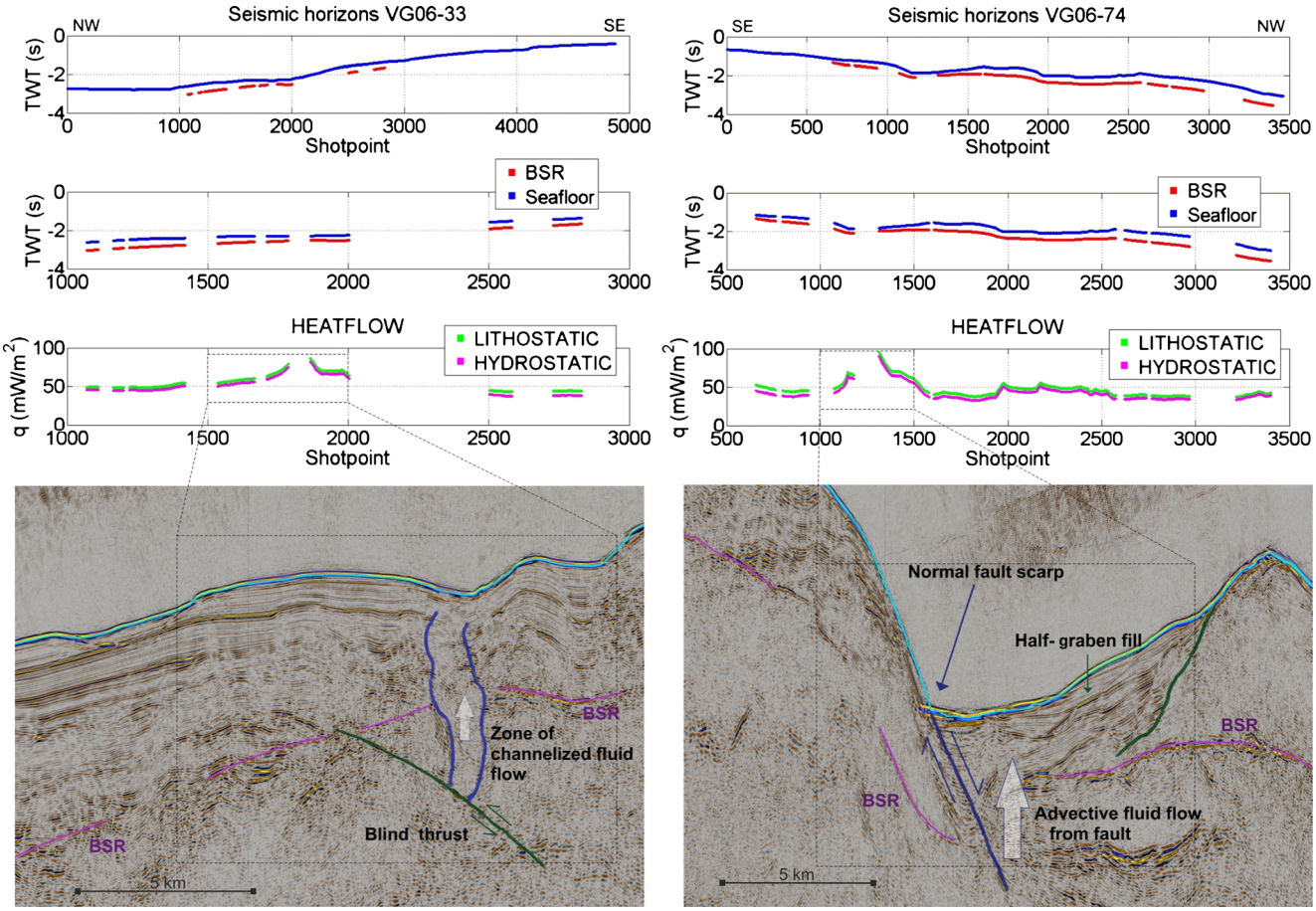

Fig. 6 Two examples of seismic profiles showing local positive anomalies of heat flow and associated tectonic structures on the forearc off Concepción, northern sector of study area. *Left* Profile VG06-33, showing BSR uplift above a blind thrust at depth. *Right* Profile VG06-74, showing BSR uplift and related elevated heat flow through half-graben sediment fill in the hanging wall of a normal fault

This is similar to that observed in the upslope part of seismic profile RC 2901-745 further north. Heat flow across Taitao Ridge, which has been interpreted as an ophiolite recently accreted to the upper plate, is well above 100 mW m^{-2}, attesting to the active tectonic nature of this environment. South of the Taitao Fracture Zone and seawards of the Golfo de Penas, heat flow computed from BSR depth is much lower (cf. southernmost data points on Fig. 4a and b), plausibly reflecting the subduction of oceanic crust of the ca. 7-Ma-old Antarctic Plate long after the passage of the Chile Ridge.

Discussion

Uncertainties in heat flow estimates

BSR-based computations of crustal heat flow need to consider uncertainties regarding underlying assumptions of gas hydrate composition, and the quality and measurement accuracy of parameters like thermal conductivity and acoustic velocity. As Brown et al. (1996) pointed out, gas hydrate stability responsible for the BSR location along the southern Chile margin is probably best explained by a more or less pure water–methane mixture. This, together with the methane-dominated gas signature of the ODP drillcores (Behrmann et al. 1992; Mix et al. 2003), speaks for a biogenic and/or thermogenic methane source of the hydrates. An important calibration for thermal conductivity and compressional wave velocity of forearc rocks is usually provided by information from boreholes, which is available for the study area from two legs of the Ocean Drilling Program (Behrmann et al. 1992; Mix et al. 2003). As pointed out above, thermal conductivities measured on rocks in the southern sector (ODP Leg 141; Behrmann et al. 1992) were higher than those in the central and northern sectors (Grevemeyer et al. 2003; Mix et al. 2003). The differences primarily reflect compositional variations of the sediments and, more importantly, a higher degree of shallow diagenesis in the vicinity of the Chile Triple Junction (see Behrmann et al. 1994).

Compressional wave velocities were taken mainly from the seismic records and errors are probably limited, especially at locations showing shallow BSRs. In the Chile Triple Junction area, drilling during ODP Leg 141 (Behrmann et al. 1992) intersected highly indurated sedimentary rocks with

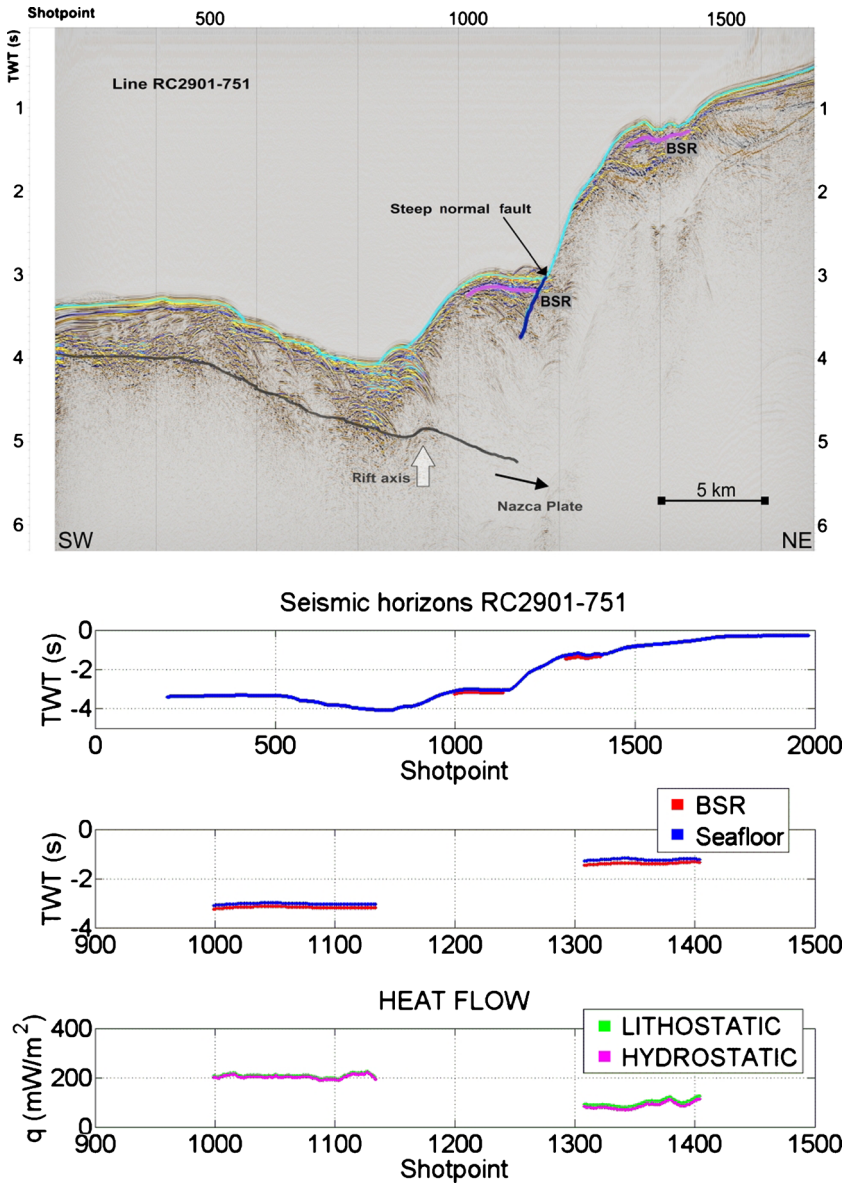

Fig. 7 Seismic profile RC 2901-751, with BSR indicative of high heat flow above the projected spreading axis of the subducted Chile Ridge. *Upper panel* Interpreted seismic profile. *Lower panels* Computed heat flow based on the seismic horizons identified for the seafloor (*blue*) and the BSR (*red*)

anomalously high compressional wave velocities at ODP Site 859 (seismic profile RC 2901-745; Fig. 5e) and Site 863 (seismic profile RC 2901-751; Fig. 7). It is difficult to accurately assess errors and discrepancies relative to the information from seismic sections. However, heat flow calculations from these two profiles may be considered as maximum estimates, as compressional wave velocity information extracted from the two seismic sections yields values lower than those measured on ODP Leg 141 drillcores (see Behrmann et al. 1992).

Ocean bottom water temperatures were taken from the World Ocean Data Base, as outlined above in the section describing the database. Local and regional variations, and variations with depth were fully accounted for in the computations. For example, typical measured seafloor temperatures are 4.2 °C at 800 m, 2.7 °C at 1,500 m and 1.8 °C at 2,500 m water depths at 36° southern latitude. Grevemeyer and Villinger (2001) pointed out that, in more general terms, heat flow calculations from BSR alone can contain uncertainties on the order of 20%. Calibrations by borehole temperature or heat probe measurements can reduce this uncertainty. In the present study this was accomplished by using direct measurements of thermal conductivity from drillcores and of temperature from drillholes, as outlined above in the materials and methods section.

BSR occurrence and water depth window

One important feature of the present findings is the distinct distribution of BSRs with respect to water depth along the Chile margin, i.e. BSR occurrence is mostly at about 2,000 m water depth. Moreover, a visual check of Figs. 3 and 4 shows

that the BSRs occur mostly in areas of very rough topography. Rough topography on the forearc is partly due to canyon incision but, much more importantly, to deformation in the vicinity of actively moving faults. For the northern part of the study area, Geersen et al. (2011a; see their Figs. 4, 5 and 7) reported that the transition from rough to smooth seafloor is typically at about 2,000 m water depth, which corresponds to 2.5–3 s TWT. While the actively deforming frontal accretionary prism is mainly located at 3,000 m water depth or more (see Fig. 8 of Geersen et al. 2011a), the forearc slope landwards from there is modified by numerous out-of-sequence thrust ridges and normal fault scarps, which are expressions of localized deformation where the slope sediment cover is underlain by older basement rock.

In the southern part of the study area, BSR occurrence is within the same water depth window (Fig. 4) and the upper, landward limit of rough topography is somewhat above the 2,000 m isobath. In the reflection seismic profiles crossing this part of the forearc, accreted strata with evidence for strong deformation occur at water depths well above 2,000 m (see Figs. 2b and 7 of the present study and, for example, Figs. 2 and 3 of Behrmann and Kopf 2001), and define a common spatial occurrence of zones of active deformation and BSRs. In principle this means that the accreted and faulted strata of the forearc are the major methane source along the whole length of the southern Chile forearc. However, the organic carbon content of the forearc and accreted trench strata is commonly rather low (ca. 0.5% or less; Behrmann et al. 1992; Mix et al. 2003), implying a very efficient process of methane migration from depth and concentration beneath the BSR (also see below).

Evidently, deformation and associated fracturing and increase in permeability probably is the key agent in facilitating methane migration from depth. In many cases this migration may be diffuse if viewed at a large scale, but the evidence from Fig. 6 suggests that it may also be individual faults that aid in channelling the fluid flow and heat flux from the forearc. In this case heat flow intensity may be roughly twice as high as the local average on both sides of the faults. The presence of seep structures (Klaucke et al. 2012) is further independent evidence that fluid flow through the forearc strata may in places be focused.

N–S gradient in BSR continuity

The data reveal that BSR occurrence is strong and laterally persistent in the south of the study area, and weaker and much more patchy in the north (compare Figs. 2 and 5). Organic carbon contents of sediments along the whole margin are relatively low, and the fill of the Chile Trench is characterized by rapidly settling, coarser terrigenous and hemipelagic sediments (Heberer et al. 2010; Geersen et al. 2011b). Indeed, there is no evidence of more slowly settling, finer-grained organic carbon-rich pelagic sediments on the subducting Nazca Plate in the northern sector of the study area, which could serve as a powerful methane source at depth and fuel gas hydrate formation near the seafloor. This is consistent with the weaker and more patchy BSR signatures in this sector.

For the immediate surroundings of the Chile Triple Junction in the south of the study area where heat flow is much higher, Brown et al. (1996) argued that the coherent BSR may result from an upward migration of the base of gas hydrate stability by about 300 m. BSR migration would cause amalgamation of isolated gas hydrate patches into one, highly reflective and continuous layer. This process would be driven by the rising geothermal gradient as the eastern flank of the Chile Ridge is becoming subducted. However, rapid upward migration of the base of the hydrate stability field would tend to leave traces such as multiple BSRs, which do not occur anywhere in the seismic sections studied. Also, the absence of multiple BSRs makes it less likely that upward BSR migration has created a non-steady state situation, which would have made calculation of heat flow from BSR depth difficult. An arguably more straightforward explanation is that vigorous fluid advection in this regime of high heat flow leads to higher methane and water flux from depth and, thus, a stronger and more continuous BSR. In some of the cores taken in ODP Leg 141 drillholes, higher hydrocarbons were detected (Behrmann et al. 1992), attesting to a contribution of thermogenic methane from depth to this part of the forearc.

The strong and continuous BSR in seismic profile RC 2901-738 (Fig. 5d) occurs in a heat flow regime of about

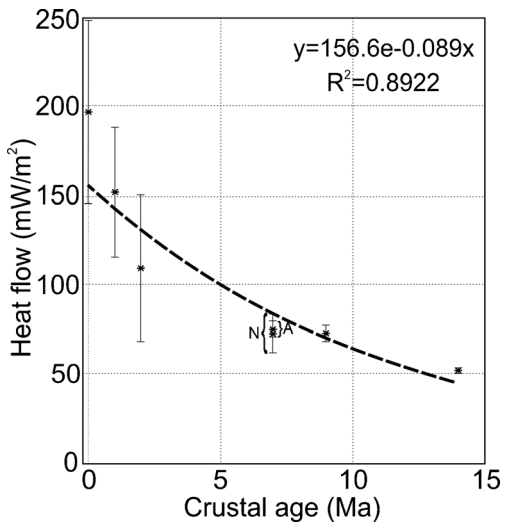

Fig. 8 Present-day forearc heat flow as a function of the age of subducted Nazca and Antarctic plate segments at the trench between 44°S and 48°S (mean heat flow for each segment between fracture zones, and one sigma standard deviation), with evidence of an exponential decay in heat flow with increasing age of the subducting plate. The two mean values for the crustal age of 7 Ma refer to the average heat flows through the subducting Nazca (*N*) and Antarctic (*A*) plates. See text for discussion

100 mW m^{-2} (Figs. 4b, 5d). This is roughly twice the average heat flow observed further north, where BSR occurrence is discontinuous. This implies that enhanced gas hydrate formation above a BSR driven by elevated heat and fluid flux from depth may already be possible at the 100 mW m^{-2} level, and would not require the strongly elevated heat flow (200–300 mW m^{-2}) observed immediately above the subducting spreading ridge further south (Figs. 4b, 5e, 5f, 7). The effect of BSR patchiness vs. continuity on assessments of gas hydrates as an energy resource (e.g. Burwicz et al. 2011) remains to be analyzed in detail. The present dataset is in principle suitable for such work (see, for example, Vargas Cordero et al. 2010b). Viewed at a larger scale and entirely qualitatively, it seems that there could be a direct link between heat flow intensity and the efficiency of gas hydrate formation in forearc sediments.

Large-scale tectonics and forearc heat flow

It is obvious from the results of this study that the subduction of the Chile Ridge and its associated oceanic spreading centre causes a major heat flow anomaly in the forearc of the overriding South American Plate. The size of the anomaly and that of the subducting spreading ridge segment between the Darwin and Taitao fracture zones correspond well (Fig. 4b). However, average heat flow in the overriding plate is not as high as one would expect above zero-age oceanic lithosphere based on thermal and subsidence models (e.g. Stein and Stein 1992). Initial heat flow predicted by Stein and Stein (1992) would be about 280–300 mW m^{-2}, and not on average 200 mW m^{-2} as shown in Fig. 8. Such deviations of heat flow intensities are known in subduction trench settings (e.g. Grevemeyer et al. 2005), and have been attributed to the cooling effect of hydrothermal circulation through normal fault systems in the subducting oceanic plate. Grevemeyer et al. (2005) argued that this effect is largely controlled by the presence or absence of a sedimentary blanket of the oceanic crust. As new oceanic crust around spreading centres is heavily faulted and not covered by sediments, the effect documented at the Chile Triple Junction may then in fact be used to quantify the cooling effect of hydrothermal circulation in this kind of tectonic setting. Indeed, this cooling effect would be strong enough to diminish heat flow from the subducting Nazca oceanic slab by as much as one third, a value derived by comparing the average 280–300 mW m^{-2} from published models (e.g. Stein and Stein 1992) with the average 200 mW m^{-2} observed above the subducting Chile Ridge (Fig. 8). This would weaken the thermal anomaly in the overriding plate accordingly. Plotting average heat flow in the forearc above older subducted Nazca and Antarctica crust (Fig. 8), there is evidently an exponential decay of this signal with time, leading to heat flow through the forearc of about 50 mW m^{-2} above 14-Ma-old subducted crust. This value is still well below the heat flow levels expected from models or heat flow measurements on open oceanic plates (Stein and Stein 1992), and implies that much of the heat generated by magmatic activity at the spreading ridge in the Nazca and Antarctic crust is removed more or less instantaneously by hydrothermal cooling. In the north of the study area where much older oceanic crust of the Nazca Plate is being subducted, the regional low values for heat flow (30–60 mW m^{-2}) come much closer to expected surface heat flow in older oceanic or continental crust (e.g. Davies and Davies 2010).

Conclusions

The findings and interpretations discussed above lead to the following main conclusions:

1. On the Chile forearc between 33° and 47° southern latitude, close spatiotemporal links exist between large-scale tectonic features and heat flow intensity. In the south, the forearc is heated from beneath by the subducting Chile Ridge, causing an approx. fourfold increase in heat flow. Absolute values and their comparison to global models and data, however, also show that there must be cooling of the crust formed at the Chile spreading ridge shortly after its formation, and before being subducted. Further north, where older Nazca Plate lithosphere is subducted beneath the South American continent, surface heat flow (30–60 mW m^{-2}) more closely matches global average values for oceanic and continental crust.
2. In the south of the study area in the vicinity of the Chile Triple Junction, the BSR marking inferred gas hydrate occurrence is continuous and strong. Further north BSRs are widespread but patchy. Rising heat flow above a subducting spreading ridge may generate a powerful methane source at depth in the subduction zone. Vigorous fluid flux then creates a strong and continuous BSR. This study provides evidence that heat flow of 100 mW m^{-2}, which is about two to three times the large-scale average of 30–60 mW m^{-2}, may already be sufficient to drive this process.
3. There is a spatial linkage between BSR and, thus, inferred gas hydrate occurrence and active deformation in the study area. Accreted and faulted strata of the forearc are the major methane source along the whole length of the southern Chile forearc. Deformation and associated fracturing and increase in permeability probably is the key agent in facilitating methane migration from depth. As these sediments are relatively poor in organic carbon, there must be a very efficient process of methane migration from depth and concentration beneath the BSR. Much of the methane migration is probably diffuse, but increased heat flow in the vicinity of individual faults implies that these can act as channels for deep-rooted fluids and heat.

Acknowledgements We are grateful to the contributors of the programme *Hidratos de gas submarinos: una nueva fuente de energía para el siglo XXI* (FONDEF Grant D00I11004), who provided the time migrated data from R/V Vidal Gormaz cruises VG02 and 06. We thank GEOMAR for the use of data from R/V Sonne cruises S0161 and SO101. Special thanks are due to Steven Cande and Stephen Lewis, who acquired the openly available data (http://www.ig.utexas.edu/sdc/) of R/V Robert Conrad Cruise RC 2901. Lucia Villar-Muñoz acknowledges tenure of a postgraduate DAAD grant, Heiner Villinger for stimulating input, and an invitation to participate in the ECORD Summer School 2011 at MARUM, Bremen, Germany. Constructive comments from two anonymous reviewers, as well as the guest editor Catherine Pierre and the journal editors were most helpful in improving the manuscript.

References

Angermann D, Klotz J, Reigber C (1999) Space-geodetic estimation of the Nazca-South America Euler vector. Earth Planet Sci Lett 171: 329–334. doi:10.1016/S0012-821X(99)00173-9

Bangs NL, Brown KM (1995) Regional heat flow in the vicinity of the Chile Triple Junction constrained by the depth of the bottom simulating reflector. In: Lewis SD, Behrmann JH, Musgrave RJ et al. (eds) Proc ODP Sci Results 141:253–258

Bangs NL, Cande SC (1997) Episodic development of a convergent margin inferred from structures and processes along the southern Chile margin. Tectonics 16:489–503. doi:10.1029/97TC00494

Bangs NL, Sawyer DS, Golovchenko X (1993) Free gas at the base of the gas hydrate zone in the vicinity of the Chile triple junction. Geology 21:905–908

Behrmann JH, Kopf A (2001) Balance of tectonically accreted and subducted sediment at the Chile Triple Junction. Int J Earth Sci 90: 753–768

Behrmann JH, Meissl S (2012) Submarine landslides, Gulf of Mexico continental slope: insights into transport processes from fabrics and geotechnical data. In: Yamada Y, Kawamura K, Ikehara K, Ogawa Y, Urgeles R, Mosher D, Chaytor J, Strasser M (eds) Submarine mass movements and their consequences. Springer, Heidelberg, pp 463–474. doi:10.1007/978-94-007-2162-1

Behrmann JH, Lewis SD, Musgrave R, Bangs N, Bodén P, Brown K, Collombat H, Didenko AN, Didyk BM, Froelich PN, Golovchenko X, Forsythe R, Kurnosov V, Lindsley-Griffin N, Marsaglia K, Osozawa S, Prior D, Sawyer D, Scholl D, Spiegler D, Strand K, Takahashi K, Torres M, Vega-Faundez M, Vergara H, Waseda A (1992) Chile Triple Junction. Proc ODP Init Rep A 141:1–708

Behrmann JH, Lewis SD, Cande S, Leg ODP, 141 Scientific Party (1994) Tectonics and geology of spreading ridge subduction at the Chile Triple Junction; a synthesis of results from Leg 141 of the Ocean Drilling Program. Geol Rdsch 83:832–852

Berndt C, Bünz S, Clayton T, Mienert J, Saunders M (2004) Seismic character of bottom simulating reflectors: examples from the mid-Norwegian margin. Mar Petrol Geol 21:723–733

Bohm M, Luth S, Echtler H, Asch G, Bataille K, Bruhn C, Rietbrock A, Wigger P (2002) The Southern Andes between 36 degrees and 40 degrees S latitude: seismicity and average seismic velocities. Tectonophysics 356:275–289

Brown KM, Bangs NL, Froelich PN, Kvenvolden KA (1996) The nature, distribution, and origin of gas hydrate in the Chile Triple Junction region. Earth Planet Sci Lett 139:471–483

Burwicz EB, Rüpke LH, Wallmann K (2011) Estimation of the global amount of submarine gas hydrates formed via microbial methane formation based on numerical reaction-transport modeling and a novel parameterization of Holocene sedimentation. Geochim Cosmochim Acta 75:4562–4576. doi:10.1016/j.gca.2011.05.029

Campos J, Hatzfeld D, Madariaga R, Lopez G, Kausel E, Zollo A, Iannacone G, Fromm R, Barrientos S, Lyon-Caen H (2002) A seismological study of the 1835 seismic gap in south-central Chile. Phys Earth Planet Interiors 132:177–195. doi:10.1016/S0031-9201(02)00051-1

Comte D, Eisenberg A, Lorca E, Pardo M, Ponce L, Saragoni R, Singh SK, Suarez G (1986) The 1985 central Chile earthquake: a repeat of previous great earthquakes in the region? Science 233:449–453. doi: 10.1126/science.233.4762.449

Contardo X, Cembrano J, Jensen A, Díaz-Naveas J (2008) Tectono-sedimentary evolution of marine slope basins in the Chilean forearc (33°30′–36°50′S): insights into their link with the subduction process. Tectonophysics 459:206–218

Contreras-Reyes E, Flueh ER, Grevemeyer I (2010) Tectonic control on sediment accretion and subduction off south central Chile: implications for coseismic rupture processes of the 1960 and 2010 megathrust earthquakes. Tectonics 29, TC6018. doi:10.1029/2010TC002734

Davies JH, Davies DR (2010) Earth's surface heat flux. Solid Earth 1:5–24

Diaz-Naveas J (1999) Sediment subduction and accretion at the Chilean convergent margin between 35° and 40°S. PhD Dissertation, University of Kiel, Kiel

Diaz-Naveas J (2007) Preliminary seismic and bathymetric results of VG06 cruise off Central Chile. In: Abstr Vol Worksh Science and Technology Issues in Methane Hydrate R&D, 5–9 March 2006, Kauai, Hawaii, p 53

Dickens GR, Quinby-Hunt MS (1994) Methane hydrate stability in seawater. Geophys Res Lett 21:2115–2118

Froelich PN, Kvenvolden KA, Torres ME, Waseda A, Didyk BM Lorenson TD (1995) Geochemical evidence for gas hydrate in sediment near the Chile triple junction. In: Lewis SD, Behrmann JH, Musgrave RJ et al. (eds) Proc ODP Sci Results 141:279–286

Ganguly N, Spence GD, Chapman NR, Hyndman RD (2000) Heat flow variations from bottom simulating reflectors on the Cascadia margin. Mar Geol 164:53–68

Geersen J, Behrmann JH, Völker D, Krastel S, Ranero CR, Diaz-Naveas J, Weinrebe W (2011a) Active tectonics of the South Chilean marine fore arc (35°S-40°S). Tectonics 30, TC3006. doi:10.1029/2010TC002777

Geersen J, Voelker D, Behrmann JH, Reichert C, Krastel S (2011b) Pleistocene giant slope failures offshore Arauco Peninsula, Southern Chile. J Geol Soc 168:1237–1248

Geersen J, Völker D, Behrmann JH, Kläschen D, Weinrebe W, Krastel S, Reichert C (2013) Seismic rupture during the 1960 Great Chile and the 2010 Maule earthquakes limited by a giant Pleistocene submarine slope failure. Terra Nova 25:472–477

Grevemeyer I, Villinger H (2001) Gas hydrate stability and the assessment of heat flow through continental margins. Geophys J Int 145: 647–660

Grevemeyer I, Diaz-Naveaz JL, Ranero CR, Villinger HW (2003) Heat flow over the descending Nazca plate in Central Chile, 32°S to 41°S: observations from ODP Leg 202 and the occurrence of natural gas hydrates. Earth Planet Sci Lett 213:285–298

Grevemeyer I, Kaul N, Diaz-Naveas JL, Villinger HW, Ranero CR, Reichert C (2005) Heat flow and bending-related faulting at subduction trenches: case studies offshore of Nicaragua and Central Chile. Earth Planet Sci Lett 236:238–248. doi:10.1016/j.epsl.2005.04.048

Grevemeyer I, Kaul N, Díaz-Naveas JL (2006) Geothermal evidence for fluid flow through the gas hydrate stability field off Central Chile - transient flow related to large subduction zone earthquakes? Geophys J Int 166:461–468

Haberland C, Rietbrock A, Lange D, Bataille K, Hofmann S (2006) Interaction between forearc and oceanic plate at the South-Central Chilean margin as seen in local seismic data. Geophys Res Lett 33, L23302. doi:10.1029/2006GL028189

Hackney RI, Echtler HP, Franz G, Götze H-J, Lucassen F, Marchenko D, Melnick D, Meyer U, Schmidt S, Tasárová Z, Tassara A, Wiedecke S (2006) The segmented overriding plate and coupling at the South-Central Chilean margin (36–42°S). In: Oncken O, Chong G, Franz G, Giese P, Götze H-J, Ramos VA, Strecker MR, Wigger P (eds) The Andes – active subduction orogeny. Springer, Berlin, pp 355–374

Heberer B, Roeser G, Behrmann JH, Rahn M, Kopf A (2010) Holocene sediments from the Southern Chile Trench: a record of active margin magmatism, tectonics, and paleoseismicity. J Geol Soc 167:539–553. doi:10.1144/0016-76492009-015

Hyndman RD, Spence GD (1992) A seismic study of methane hydrate marine bottom-simulating-reflectors. J Geophys Res 97:6683–6698

Kaul N, Rosenberger A, Villinger H (2000) Comparison of measured and BSR-derived heat flow values, Makran accretionary prism, Pakistan. Mar Geol 164:37–51

Kayen RE, Lee HJ (1991) Pleistocene Slope Instability of gas hydrate-laden sediment on the Beaufort Sea Margin. Mar Geotechnol 10:125–141

Klaucke I, Weinrebe W, Linke P, Kläschen D, Bialas J (2012) Sidescan sonar imagery of widespread fossil and active cold seeps along the central Chilean continental margin. Geo-Mar Lett 32(5/6):489–499. doi:10.1007/s00367-012-0283-1

Kukowski N, Oncken O (2006) Subduction erosion – the "normal" mode of fore-arc material transfer along the Chilean Margin? In: Oncken O, Chong G, Franz G, Giese P, Götze H-J, Ramos VA, Strecker MR, Wigger P (eds) The Andes – active subduction orogeny. Springer, Berlin, pp 217–236

Kvenvolden KA (1998) A primer on the geological occurrence of gas hydrate. In: Henriet J-P, Mienert J (eds) Gas hydrates. Relevance to world margin stability and climate change. Geol Soc Spec Publ 137:9–30

Lomnitz C (1970) Major earthquakes and tsunamis in Chile during the period 1535 to 1955. Geol Rdsch 59:938–960. doi:10.1007/BF02042278

Maksymowicz A (2013) Reestablishment of an accretionary prism after the subduction of a spreading ridge—constraints by a geometric model for the Golfo de Penas, Chile. Geo-Mar Lett 33(5):345–355. doi:10.1007/s00367-013-0331-5

Mienert J, Posewang J, Baumann M (1998) Gas hydrates along the northeastern Atlantic margin: possible hydrate-bound margin instabilities and possible release of methane. In: Henriet J-P, Mienert J (eds) Gas hydrates. Relevance to world margin stability and climate change. Geol Soc Spec Publ 137:275–291

Milkov AV (2004) Global estimates of hydrate-bound gas in marine sediments: how much is really out there? Earth-Sci Rev 66:183–197

Mix AC, Tiedemann R, Blum P et al (2003) Proc Ocean Drilling Program Initial Reports, vol 202. Ocean Drilling Program, College Station, TX

Morales E (2003) Methane hydrates in the Chilean continental margin. Electron J Biotechnol 6(2). http://ejb.ucv.cl/content/vol6/issue2/issues/1/

Rehak K, Strecker MR, Echtler HP (2008) Morphotectonic segmentation of an active forearc, 37°–41°S, Chile. Geomorphology 94:98–116

Reichert C, Schreckenberger N, SPOC Team (2002) Fahrtbericht SONNE - Fahrt SO-161 Leg 2&3 SPOC, Subduktionsprozesse vor Chile - BMBF-Forschungsvorhaben 03G0161A-Valparaíso 16.10.2001-Valparaíso 29.11.2001. Bundesanst für Geowiss und Rohstoffe, Hannover

Ruegg JC, Rudloff A, Vigny C, Madariaga R, de Chabalier JB, Campos J, Kausel E, Barrientos S, Dimitrov D (2009) Interseismic strain accumulation measured by GPS in the seismic gap between Constitución and Concepción in Chile. Phys Earth Planet Interiors 175:78–85. doi:10.1016/j.pepi.2008.02.015

Stein CA, Stein S (1992) A model for the global variation in oceanic depth and heat flow with lithospheric age. Nature 359:123–129

Tasárová Z (2007) Towards understanding the lithospheric structure of the southern Chilean subduction zone (36°S–42°S) and its role in the gravity field. Geophys J Int 170:995–1014

Tebbens SF, Cande SC (1997) Southeast Pacific tectonic evolution from early Oligocene to Present. J Geophys Res Solid Earth 102:12061–12084. doi:10.1029/96JB02582

Vargas Cordero I (2009) Gas hydrate occurrence and morphostructures along the Chilean margin. Dissertation. University of Trieste, Trieste

Vargas Cordero I, Tinivella U, Accaino F, Loreto MF, Fanucci F, Reichert C (2010a) Analyses of bottom simulating reflections offshore Arauco and Coyhaique (Chile). Geo-Mar Lett 30(3/4):271–281. doi:10.1007/s00367-009-0171-5

Vargas Cordero I, Tinivella U, Accaino F, Loreto MF, Fanucci F (2010b) Thermal state and concentration of gas hydrate and free gas of Coyhaique, Chilean Margin (44°30′S). Mar Petrol Geol 27:1148–1156. doi:10.1016/j.marpetgeo.2010.02.011

Vargas Cordero I, Tinivella U, Accaino F, Fanucci F, Loreto MF, Lascano ME, Reichert C (2011) Basal and frontal accretion processes versus BSR characteristics along the Chilean margin. J Geol Res 2011:846101. doi:10.1155/2011/846101

Villinger H, Tréhu AM, Grevemeyer I (2010) Seafloor marine heat flux measurements and estimation of heat flux from seismic observations of bottom simulating reflectors. In: Riedel M, Willoughby EC, Chopra S (eds) Geophysical characterization of gas hydrates. Society of Exploration Geophysicists, Tulsa, OK, pp 279–300

Völker D, Wiedicke M, Ladage S, Gaedicke C, Reichert C, Rauch K, Kramer W, Heubeck C (2006) Latitudinal variation in sedimentary processes in the Peru-Chile Trench off Central Chile. In: Oncken O, Chong G, Franz G, Giese P, Götze H-J, Ramos VA, Strecker MR, Wigger P (eds) The Andes – active subduction orogeny. Springer, Berlin, pp 193–216

Völker D, Geersen J, Behrmann JH, Weinrebe WR (2012) Submarine mass wasting off southern central Chile: distribution and possible mechanisms of slope failure at an active continental margin. In: Yamada Y, Kawamura K, Ikehara K, Ogawa Y, Urgeles R, Mosher D, Chaytor J, Strasser M (eds) Submarine mass movements and their consequences. Springer, Heidelberg, pp 379–389. doi:10.1007/978-94-007-2162-3_34

von Huene R, Corvalán J, Flueh ER, Hinz K, Korstgard J, Ranero CR, Weinrebe W, Scientists CONDOR (1997) Tectonic control of the subducting Juan Fernández Ridge on the Andean margin near Valparaiso, Chile. Tectonics 16:474–488